대형콘크리트구조물의 수화열 예측 및 균열제어 연구

Temperature Analysis and Crack Control of Large Scale Massive Concrete Structures Due to Hydration Heat

오병환* 백신원**
Oh, Byung Hwan, Paik, Shin Won

요 약

최근에 우리나라에서는 매스콘크리트 구조물의 시공시 심각한 균열이 발생하는 사례가 빈번히 일어나고 있다. 이러한 매스콘크리트에서 균열의 주원인은 시멘트의 수화반응에 의한 수화열때문인 것으로 알려졌다. 매스콘크리트의 경우 물과 시멘트의 화학반응에 의해 발생하는 수화열로 인해 구조물의 내부에 높은 온도가 유발되며 이 때 내외부의 온도차에 의해 열응력이 발생하게 된다. 이 열응력의 크기와 방향은 시멘트의 종류와 함유량, 부재의 크기 및 경계조건, 주변의 대기온도 분포 등에 크게 영향을 받는다.

본 연구에서는 매스콘크리트 구조물의 온도분포 및 열응력을 예측할 수 있는 해석프로그램을 개발하는데 그 목적이 있다. 또한, 매스콘크리트의 온도 및 열응력 특성을 규명하기 위한 교량의 기초 및 기둥 모형에 대한 현장실험을 실시하였다. 이 때 시험체에서의 각 측정점의 온도 및 변형량은 자동으로 측정 및 저장되어지는 Data Logger System을 이용하였다.

본 연구에서는 수화열에 의한 콘크리트의 강도발현을 좀 더 정확하게 추정하기 위하여 성숙도 개념을 새로이 해석에 도입하였다. 또한, 새로운 개념으로서 소위 균열지수 개념을 고안하여 해석프로그램을 개발하였다. 그리고 콘크리트의 크리프와 건조수축의 영향을 해석에 고려하였다. 본 연구결과 매스콘크리트의 실험치와 해석치가 비교적 잘 일치하는 결과를 보였다. 따라서, 본 연구는 매스콘크리트의 수화열에 의한 균열을 예측하고 억제하는데 중요한 토대를 제공하며 앞으로 매스콘크리트 구조물의 합리적인 해석 및 설계를 가능하게 한 것으로 사료된다.

ABSTRACT

Recently, serious cracking problems have been reported in this country in the course of actual massive concrete construction. Major cause of this cracking is found to be mainly due to the hydration heat of mass concrete. The hydration heat arising from the chemical reaction of cement with water causes temperature differentials between inside and outside of a structural member and these temperature differentials induce thermal stresses. The magnitude and direction of ther-

* 정회원, 서울대학교 토목공학과 교수
** 정회원, 안성산업대학교 토목과 강사

• 본 논문에 대한 토의를 1995년 4월 30일까지 학회로 보내주시면 1995년 6월호에 토의회답을 게재하겠습니다.

mal stresses are much dependent upon the types and amount of cement, the size and boundary conditions of the member, and also ambient temperature distributions.

To find the heat evolution law of ordinary cement, a series of tests for adiabatic temperature rise were conducted. A field test has been also conducted to simulate actual construction of footing and column of a bridge. The measurements of temperatures and strains at various points of the test members have been automatically done and stored in the computer.

The maturity concept is introduced to account for accurate strength development due to hydration. The present study indicates that the effect of shrinkage is significant in the resulting stresses while the creep of concrete influences little the thermal stresses. Comparisons of present theory with experimental data show reasonably good correlation. The present study allows realistic analysis and design of massive concrete structures to prevent cracking and detrimental effects.

Keywords : mass concrete, hydration heat, thermal stresses, heat transfer, adiabatic temperature rise, large scale structures, temperature distribution.

1. INTRODUCTION

Large scale concrete structures have been increasingly built at various locations in the world. One of the major problems in the construction of these large concrete structures is to control efficiently the great hydration heat arising in massive concrete. The hydration heat arising from the chemical reaction of cement with water causes temperature differentials between inside and outside of a structural member and these temperature differentials induce thermal stresses(1-5, 10-17). The magnitude and direction of thermal stresses are much dependent upon the types and amount of cement, the size and boundary conditions of the member, and also ambient temperature distributions(1-5).

The purpose of the present study is therefore to develop an analytical model that can predict the temperature distributions and thermal stresses of any massive concrete structures. The creep and shrinkage of concrete may seriously influence the thermal stresses. The effects of creep and shrinkage of concrete are, therefore, included in the present analysis. The aging of concrete and thus strength development phenomenon is also considered. The ACI, CEB and BP models for creep and shrinkage prediction are incorporated in the present program.

The maturity concept is introduced to account for accurate strength development due to hydration(12). A so-called cracking index concept is also devised to figure out the cracking regions in a structure.

To find the heat evolution law of ordinary cement, a series of tests for adiabatic temperature rise were conducted. A field test has been also conducted to simulate actual construction of footing and column of a bridge.

2. FINITE ELEMENT FORMULATION FOR TEMPERATURE AND THERMAL STRESS ANALYSES

2.1 Theoretical Formulation

For the development of a finite element scheme either a galerkin formulation of the

heattransfer problem. In the variational formulation a functional Π is defined such that when invoking the stationarity of Π,

$$\int\{\delta T'\}^T[k]\{T'\}dV = \int\delta T(g+q^I)dV+\int\delta Tq^C dS^C+\int\delta Tq^R dS^R \quad (1)$$

where

$$\{T'\} = [\frac{\partial T}{\partial x}\ \frac{\partial T}{\partial y}\ \frac{\partial T}{\partial z}]^T$$

$$[k] = \begin{bmatrix} k_x & 0 & 0 \\ 0 & k_y & 0 \\ 0 & 0 & k_z \end{bmatrix}$$

$$q^I = \rho c \frac{\partial T}{\partial t}$$

$$q^c = h_c (T_e - T^S)$$

$$q^R = h_r (T_r - T^S)$$

where q^I is the rate of heat generated per unit volume of the heat capacity effect, h is the convection coefficient, T_r is the temperature of the external radiative source and h_r is a coefficient.

We consider an isoparametric solid element in three dimensions and interpolate temperature T and temperature gradient T' along an element from nodal temperatures {T}. Therefore, the equilibrium equations of the element assemblage corresponding to the global nodal temperatures are

$$[C]\{\dot{T}\} + [K]\{T\} = \{R\} \quad (2)$$

where

thermal stiffness matrix :

$$[K] = [K^k] + [K^c] + [K^r]$$

thermal load vector :

$$\{R\} = \{R_g\} + \{R_c\} + \{R_r\}$$

heat capacity matrix :

$$[C] = \sum_{i=1}^{n}\int[N]^T \rho c[N]\, dV$$

conductivity matrix :

$$[K^k] = \sum_{i=1}^{n}\int[B]^T [k][B]\, dV$$

convection matrix :

$$[K^c] = \sum_{i=1}^{n}\int[N]^T h_c[N]dS^S$$

radiation matrix :

$$[K^r] = \sum_{i=1}^{n}\int[N]^T h_r[N]dS^R$$

heat generation load vector :

$$\{R_g\} = \sum_{i=1}^{n}\int[N]^T g\, dV$$

convection load vector :

$$\{R_c\} = \sum_{i=1}^{n}\int[N]^T h_c T_e\, dS^C$$

radiation load vector :

$$\{R_r\} = \sum_{i=1}^{n}\int[N]^T h_r T_r\, dS^R$$

In thermal problems, a time-varying solution can be obtained by direct temporal integration. In this study, A two time level recurrence scheme is applied to thermal transient analysis. In this scheme it is assumed that the temperature varied linearly in a discrete time interval, Δt, from t_n to time $t_{n+1}=t_n+\Delta t$. We consider two temperature states, separated by time increment Δt, $\{T\}_n$ and $\{T\}_{n+1}$. Using generalized trapezoidal rule, the temperature at time $t_{n+\alpha}=t_n+\alpha\Delta t$ is written as

$$\{T\}_{n+\alpha} = \{T\}_n + \alpha\Delta t\{\dot{T}\}_{n+\alpha} \quad \alpha\in(0,1) \quad (3)$$

where α is a constant which is chosen to yield optimum stability and accuracy properties.

Rewriting Eq.(2) for time $t_{n+\alpha}$

$$[C]_{n+\alpha}\{\dot{T}\}_{n+\alpha} + [K]_{n+\alpha}\{T\}_{n+\alpha} = \{R\}_{n+\alpha} \quad (4)$$

The time derivative of temperature in Eq.(3) is introduced into Eq.(4). The result is

$$([C]_{n+\alpha}+\alpha\Delta t[K]_{n+\alpha})\{T\}_{n+\alpha}=\alpha\Delta t\{R\}_{n+\alpha}+[C]_{n+\alpha}\{T\}_n \quad (5)$$

Solving Eq.(5) for $\{T\}_{n+\alpha}$, the temperature at time t_{n+1} is finally given by

$$\{T\}_{n+1}=\frac{1}{\alpha}\{T\}_{n+\alpha}+(1-\frac{1}{\alpha})\{T\}_n \quad (6)$$

The relation between strain and displacement is a key ingredient in the formulation of finite elements for stress analysis problems. In the present section we consider general strain-displacement relations in Cartesian coordinates. Then, the equilibrium equation of the element assemblage corresponding to the global nodal d.o.f. {D} is

$$[K]\{D\}=\{R\} \quad (7)$$

where

stiffness matrix,

$$[K]=\sum_{i=1}^{n}\int[B]^T[E][B]dV$$

load vector,

$$\{R\}=\{R_\rho\}-\{R\sigma\}+\{R_F\}+\{R_P\}$$

initial strain load vector,

$$\{R_\rho\}=\sum_{i=1}^{n}\int[B]^T[E]\{\varepsilon_0\}dV$$

initial stress load vector,

$$\{R_\sigma\}=\sum_{i=1}^{n}\int[B]^T\{\sigma_0\}dV$$

body force load vector,

$$\{R_F\}=\sum_{i=1}^{n}\int[N]^T\{F\}dV$$

external load vector,

$$\{R_P\}=\sum_{i=1}^{n}\{P\}$$

The initial strain in Eq.(7) implies the non-mechanical strain and is composed of the following components

$$\{\varepsilon_0\}=\{\varepsilon_c\}+\{\varepsilon_s\}+\{\varepsilon_a\}+\{\varepsilon_T\} \quad (8)$$

where

$\{\varepsilon_c\}$ = creep strain vector

$\{\varepsilon_s\}$ = shrinkage strain vector

$\{\varepsilon_a\}$ = aging strain vector

$\{\varepsilon_T\}$ = temperature strain vector

$$= \alpha_c(\sum N_i\Delta T_i)[1\ 1\ 1\ 0\ 0\ 0]^T$$

where ΔT_i is a relative temperature of each node of the element and α_c is a thermal expansion coefficient.

As is well known, the strength of a given concrete mixture, which has been properly placed, consolidated and cured, is a function of its age and temperature history. At early ages, temperature has a dramatic effect on strength development. This temperature dependence presents problems in trying to estimate the in-place strength based on strength development data obtained under standard laboratory conditions.

The term "maturity" was for the first time linked to the product of time and temperature. Thus maturity is computed from the temperature history using the following equation.

$$M=\int_0^t(T-T_0)\,dt \quad (9)$$

where, M : maturity at age t

T : element temperature

T_0 : datum temperature

This equation has become known as the Nurse-Saul function. Generally, a value of $-10℃$ for the datum temperatrue has been used in subsequent applications of the Nurse-Saul function. Then, the strength of concrete can be

written as a function of the logarithm of maturity. Therefore, compressive strength at any time is written as follows.

$$f'_c(M) = a + b \log M \qquad (10)$$

ACI Committee 209R recommends the following formula which was developed by Pauw in 1960,

$$E_c(M) = 0.1346 \sqrt{\rho^3 f'_c(M)} \qquad (11)$$

where ρ is the density of concrete in kg/m^3 and $f'_c(M)$ is the compressive strength in kg/cm^2.

2.2 Flow Diagram

In this study, we develop two programs which analyze temperature and thermal stress for the mass concrete structures(6-9). The two programs developed in this study were written in FORTRAN language. An program named "HYTAM1"(Hydration Temperature Analysis of Mass Concrete Structures) solves for transient temperature using(Fig. 1) heat-flow in the mass concrete structures(6-9).

The "HYTAM2" is a thermal stress analysis program for the mass concrete structures using the temperature results from "HYTAM1". In the program "HYTAM2", a following procedure for the incremental analysis of solid concrete structures considering maturity is incorporated. The time dependent effects due to creep, shrinkage, and aging of concrete, and temperature variations are included.

The total incremental strain, $\Delta\varepsilon$, from time t to time $(t+\Delta t)$ is shown in Eq.(1).

$$\Delta\varepsilon = \Delta\varepsilon^{n} + \Delta\varepsilon^{nm} \qquad (1)$$

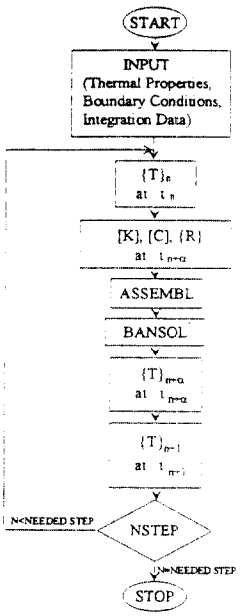

Fig. 1 Flow diagram of temperature analysis program

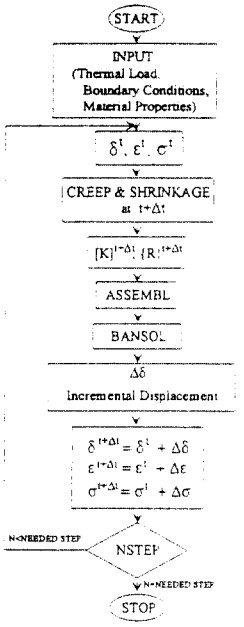

Fig. 2 Flow diagram of thermal stress analysis program

where $\Delta\varepsilon^{m}$ is an incremental mechanical strain vector, $\Delta\varepsilon^{nm}$ is an incremental non-mechanical strain vector including thermal strain($\alpha\,\Delta T$), α is a coefficient of expansion, ΔT is an incremental temperature $T^{t+\Delta t}-T^{t}$, and the incremental stress is as follows.

$$\Delta\sigma = E\,(\Delta\varepsilon - \Delta\varepsilon^{nm}) \qquad (2)$$

where E is a stress-strain matrix including maturity of element. Total displacement, total strain and total stress are written as follows.

$$\delta^{t+\Delta t} = \delta^{t} + \Delta\delta \qquad (3a)$$

$$\varepsilon^{t+\Delta t} = \varepsilon^{t} + \Delta\varepsilon \qquad (3b)$$

$$\sigma^{t+\Delta t} = \sigma^{t} + \Delta\sigma \qquad (3c)$$

where $\delta^{t+\Delta t}$ is a nodal displacement vector at time $t+\Delta t$.

Flow diagram of this thermal stress analysis program is shown in Fig.2.

3. TESTS ON HYDRATION HEAT OF MASS CONCRETE

3.1 Design and Fabrication of Test Members

In the mass concrete structures such as large footing and pier of a bridge, when they are placed, great amount of hydration heat by cement occurs. Such temperature differences may cause high thermal stresses. These thermal stresses may cause cracking in mass concrete structures and thus it gives serious problems in structures.

In this study, we modeled the test member for the pier footing and column shape, which can bring about sufficient hydration heat by cement. That test model is as shown in Fig.3. Footing is 3m×2m×1m and column is 2m×1m×1m. In addition, in the test of temperature distribution and thermal stress by hydration heat of mass concrete structure, the reinforcements of structures is also very important because they restrain the cracks. But, in this test, we designed the footing and column without consideration of loads. So we adopt 0.15% of member area as the minimum reinforcement ratio recommended by ACI As shown in Fig.4, we used D16 as longitudinal steel of footing and D19 as longitudinal steel of column. And we used D10 as the stirrup of both footing and column. All reinforcements used in this test are the high strength steel (SD40) with the yield strength of 4,000kg /cm^2.

In the test of mass concrete structure, it is important to locate the temperature gauge and strain gauge. Because the cross section of mass concrete structure is symmetric, we embedded all the gauges in guarter cross section of test members.

Fig.5a shows the location of temperature gauges and the number of these gauges. And Fig.5b shows the location of strain gauges and the number of these gauges, where T, M, and B mean top, middle, and bottom of the test member respectively.

The mix proportion of the present test mem-

Table 1 Mix proportion of concrete(kg/ m^3)

Cement content	Water	Fine aggregate	Coarse Aggregate	Admixure
382	190	768	942	0.76

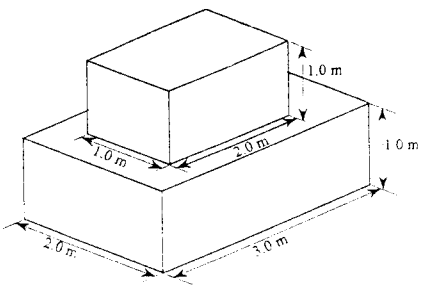

Fig. 3 The size of test member(m)

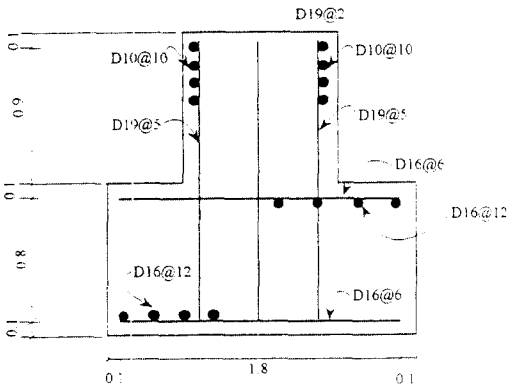

Fig. 4 Design of reinforcement(m)

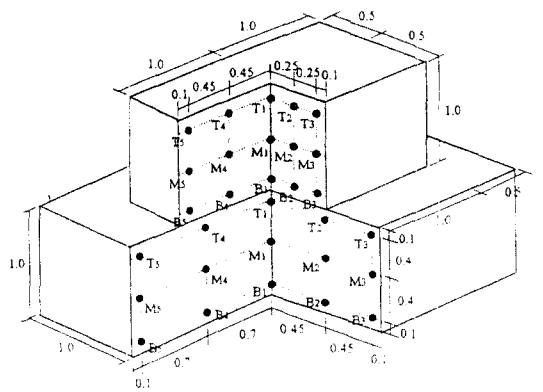

Fig. 5(a) The location and number of temperature gauges(m)

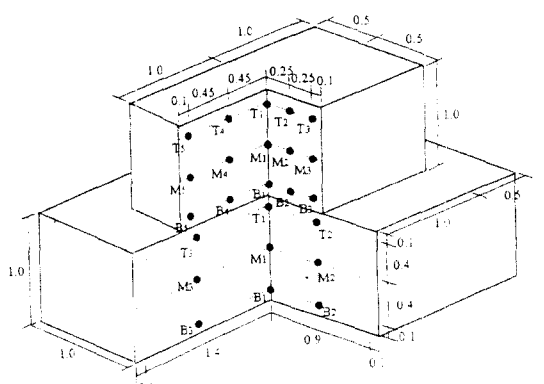

Fig. 5(b) The location and number of strain gauges(m)

ber is shown in Table 1, where unit cement content is 382kg/m^3, sand to total aggregate ratio is 45%, water-cement ratio is 49.8%.

3.2 Test Methods and Measurements

Temperatures and strains at various locations were automatically measured using the Data Logger System. When two days passed after placing concrete, we removed the forms of footing, and established the temperature gauges and strain gauges at column. Then we placed concrete at column, and measured temperature and strain of column like the previous method of footing. On the other hand, we measured continuously temperature and strain of footing in order to predict the influence of placing the column concrete.

In the analysis of mass concrete temperature, adiabatic rising temperature curve is needed. So, in this study, we made cubic specimen to get the adiabatic temperature-rise curve. First, in order to make the cubic block (50cm×50cm×50cm), we made the form (90cm×90cm×90cm) of wood panel. And all surfaces of specimen were insulated by polystyrol with a thickness of 20cm. Although the cubic concrete specimen is enclosed by polystyrol with a thickness of 20cm, the interior of the cubic specimen cannot be kept completely adiabatic because of heat release to the outside through polystyrol. Therefore, we predicted the adiabatic temperature-rise curve indirectly by time-dependent analysis about the cubic specimen.

The magnitude of the stress distributions generated by heat of hydration depends strongly on the concrete modulus of elasticity. Therefore, in order to consider this effects, we made 24 cylinders(10cm×20cm) with the same mixture as test member to measure the time-dependent change of elastic modulus and strength.

4. TEST AND ANALYSIS RESULTS

4.1 Introduction

The properties of concrete and subsoil used in this analysis as input data are shown in Table 2. In this analysis, a 1/4 model of the test member is used due to the symmetry. The boundary condition on the symmetric plane and on the outside faces of the subsoil are adiabatic conditions. The finite element mesh model is shown in Fig.6. The actual temperatures of the atmosphere and the subsoil varied day by day, but the mean temperatures were used for atmosphere and subsoil, i.e., 23℃ and 22℃, respectively. The temperature at the time of placing was about 30℃. The thermal properties of footing concrete are the same as the column concrete.

Though the cubic specimen is enclosed by polystyrol, the exterior cannot be kept completely adiabatic condition. Therefore, we predicted the adiabatic temperature rise equation indirectly by temperature analysis for the cubic specimen. That is, we obtained the adiabatic temperature rise equation through analysis altering thermal properties and boundary conditions. The equation of adiabatic temperature rise which is obtained from this analysis is witten as follows.

$$T = 48(1 - e^{-3.2t}) \qquad (4)$$

To calculate the heat generation rate per unit volume and time, Eq.(4) was differentiated with respect to time. So, this analysis used the following heat generation rate per unit volume and time.

$$q = 6.4\,\rho\,c\,e^{-0.133t} \qquad (5)$$

where ρ is the unit weight of the concrete, c is the specific heat of the concrete, and t is the aging of the concrete in hours.

In this analysis, it is assumed that sliding between the bottom of the footing and the subsoil does not occur. We used the elastic modulus of the concrete obtained from the test at each time step. It is assumed that the elastic modulus of the subsoil is $1.3\times10^{7}(kg/m^{2})$. We assume that coefficient of expansion of both the concrete and the subsoil is 1.0×10^{-5}, and Poisson' ratios of the concrete and the subsoil are 0.2, 0.4, respectively. This analysis considered the creep and shrinkage recommended by ACI.

Table 2 Properties of the concrete and the subsoil

Properties / Type	Heat conductivity (kcal/mh℃)	Specific heat (kcal/kg℃)	Unit weight (kg/m³)	Heat convectivity (kcal/m²h℃)
Concrete	2.2	0.235	2320	9.0
Subsoil	1.06	0.49	1700	9.0

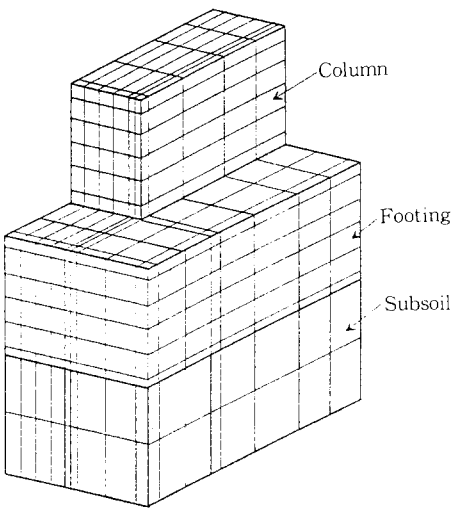

Fig. 6 Finite element mesh of the test member

4.2 Comparisons

4.2.1 Temperature Distributions

Fig.7 shows the measured and analytical tem-

peratures of the footing of the test member. The analyzed temperatures of bottom and middle were the same as the experimentally measured temperatures but the analyzed temperature at the bottom of the footing was higher than the measured one. The reason for the difference of the top is the difference in the atmospheric temperature variance. It is known that the top temperature of footing is influenced by concrete placement of column.

Fig.8 shows the measured and analytical temperatures of the column of the test member.

As shown in figures, it is recognized that the heat generation rate of the concrete is very fast. This reason is that the domestic cement is more faster. Since the domestic cement hydrates rapidly than the foreign cement, much hydration heat is induced at the early age. Therefore, we have to be careful to control initial hydration heat.

4.2.2 Strain Distributions

Fig.9 shows the measured and analytical strains of the footing of the test member. From the results, it is seen that the strain of the top is larger than the bottom of the footing.

Fig.10 shows the measured and analytical strains of the column of the test member.

The measured strain distributions fluctuate somewhat but the analyzed results are smooth. Maximum strain shows at the observation poin-

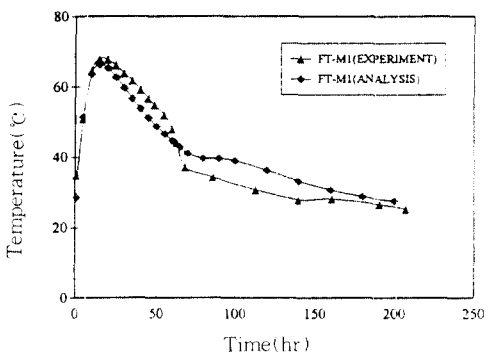

Fig. 7 Comparison of experimental and analytical temperature distributions(middle point 1 of footing)

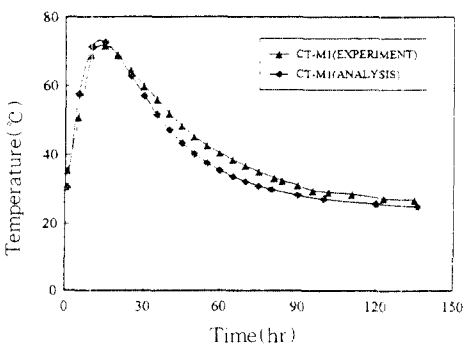

Fig. 8 Comparison of experimental and analysis temperature distributions(middle point 1 of column)

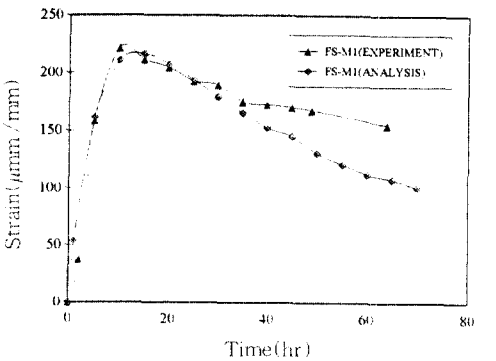

Fig. 9 Comparison of experimental and analytical strain distributions(middle point 1 of footing)

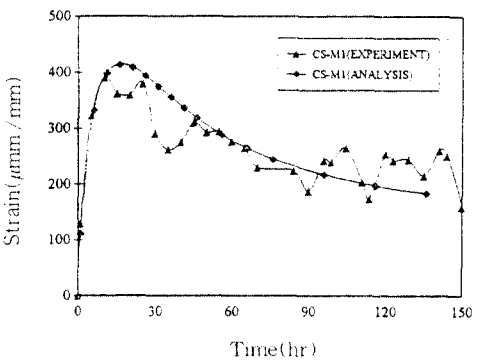

Fig. 10 Comparison of experimental and analytical strain distributions(middle point 1 of column)

t 4 of the column. Though the temperature of the footing and the column is similar, the strain of the column is greater than that of the footing.

4.2.3 Stress Results

In order to predict cracking in the mass concrete structures, a thermal stress analysis must be performed after a temperature analysis. In this study, a stress analysis for the test member was performed based on the temperature distributions considering the creep and shrinkage of the concrete.

Fig.11 shows the distributions of maximum principal stress at the observation points. In the footing, only compressive principal stress occurs. But, in the column, tensile principal stress occurs at B3, B5, M3, M5, T3, and T5. And, maximum tensile stress occurs at 28 hours after concrete placement, the magnitude of this is about 17kg/cm^2. Such principal stresses are significant and can induce cracking in the concrete at early ages.

From these results, it is known that compressive stress is induced in the interior of the column, but tensile stress is induced in the exterior.

The analyses do provide a means of assessing the relative risk of cracking for the mass concrete structures. To assess the significance of the induced thermal stresses, the maximum principal tensile stresses are compared with the tensile strength of the concrete. The cracking index concept is introduced to examine the possibility of the cracks induced by thermal stresses. Because of the significant stress distribution in the outer of the column, the modulus of rupture f_r will be used as the most appropriate measure of the tensile strength of the concrete. Therefore, the cracking index, I_c which is the ratio of the induced tensile stress against flexural tensile strength is written as follows.

$$I_c = \frac{\sigma_t(M)}{f_r(M)} \tag{6}$$

where f_r is flexural tensile strength and σ_t is tensile stress intensity of actual structure. If we assume that the modulus of rupture is about 150% of the splitting tensile strength, the cracking index of Eq.(6) is written as follows again.

$$I_c = \frac{\sigma_t(M)}{1.5f'_{sp}(M)} \tag{7}$$

where $f'_{sp}(M)$ is the splitting tensile strength. According to the result of this analysis, the cracking indices of all the points were less than 1.0, which were confirmed by experimental results.

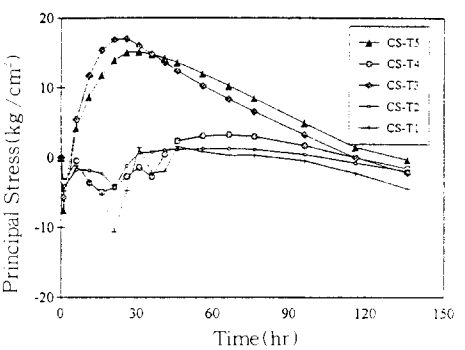

Fig. 11 Principal stress distributions(at top points of column)

5. CONCLUSION

The purpose of the present study is to develop an analytical model that can predict the temperature distributions and thermal stresses of any massive concrete structures. The creep and shrinkage of concrete may seriously influence the thermal stresses. The effects of

creep and shrinkage of concrete are, therefore, included in the present analysis. The aging of concrete and thus strength development phenomenon is also considered. The ACI, CEB and BP models for creep and shrinkage prediction are incorporated in the present program.

The maturity concept is introduced t account for accurate strength development due to hydration(12). A so-called cracking index concept is also devised to figure out the cracking regions in a structure.

To find the heat evolution law of ordinary cement, a series of tests for adiabatic temperature rise were conducted. A field test has been also conducted to simulate actual construction of footing and column of a bridge.

The measurements of temperatures and strains at various point of the test members have been automatically done and stored in the computer.

The salient feature of the present study is that a new concyept of maturity was introduced and also a new concept of cracking index was introduced which are very important especially at young concrete. Comparisons of present theory with experimental data show reasonably good correlation. The present study allows realistic design and construction of massive concrete structures.

Acknowledgement

This research was supported by KOSEF in 1994.

참 고 문 헌

1. S. J. Thurston, "Thermal Stresses in Concrete Structures," Reaserch Report, University of Canterbury Christchurch, New Zealand, 1978.

2. Dunstan, M. R. H. and Mitchell, P. B., "Results of a Thermocouple Study in Mass Concrete in the Upper Tamar Dam," Institution of Civil Engineers, London Proceedings, V.60, 1976, pp.27-52.

3. Neville, Properties of Concrete, 3rd Edition, 1981.

4. Nobuhiro Machida and Kazuo Uehara, "Nonlinear Thermal Stress Analysis of a Massive Concrete Structure," Computer & Structures, Vol.26, No.1/2, 1987, pp.287-296.

5. Fernando A. Branco, "Heat of Hydration Effects in Concrete Structures," ACI Materials JOURNAL, V.89, No.2, March-April, 1992.

6. M. Necati OZISIK, Heat Transfer(A Basic Approach), McGraw-Hill, 1985.

7. K. J. Bathe, Finite Element Procedures in Engineering Analysis, Prentice Hall, 1982.

8. R. D. Cook, Concepts and Application of Finite Element Analysis, John Wiley & Sons, 1989.

9. F. Damjanic and D. R. J. Owen, "Practical Considerations for Thermal Transient Finite Element Analysis using Isoparametric Elements," Nuclear Engineering and Design 69, 1982, pp.109-126.

10. V. M. Malhotra, N. J. Carino, Handbook on Nondestructive Testing of Concrete, CRC Press, 1991.

11. 김진식, 정재동 외 4인, "고강도콘크리트 단열온도 상승에 관한 실험적연구", 한국콘크리트학회 학술발표논문집, 제6권1호, 1994, 5. pp.209-214.

12. 오병환, 이명규 외 5인, "성숙도를 고려한 콘크리트의 강도예측에 관한연구", 한국콘크리트학회 학술발표회 논문집, 제6권 2호, 1994. 11. pp. 83-86.

13. 최계식, 양주경, 최영돈, 최고일, "수화열 계측 및 파이프 쿨링사례", 한국콘크리트학회 학술발표회 논문집, 제6권 2호, 1994. 11. pp.381-386.

14. 오병환, 백신원 외 2인, "현장조건을 고려한, 콘크리트 기초 및 교각구조의 온도 및 열응력에 관한 실험연구" 한국콘크리트학회 학술발표회논문집, 제6권 1호, 1994. 5. pp.233-237.

15. 이장화, 변근주, "매스콘크리트수화발열 특성의 정량화를 위한 실험적연구", 한국콘크리트학회 학술발표회 논문집, 제6권 1호, 1994. 5. pp. 238-242.

16. 이하성, 정상진, 정헌수 외 2인, "매스콘크리트의 고강화에 관한 실험적 연구", 한국콘크리트학회 학술발표회, 제6권 2호, 1994. 11. pp.175-179.

17. 오병환, 백신원, "매스콘크리트 구조의 열응력해석에서의 크리프 및 건조수축효과", 대한토목학회 논문집, 제14권 제1호, 1995. 1. pp.1-12.

(접수일자 : 1994. 10. 7)